Taylor & Francis
Taylor & Francis Group

Applied Earth Science

Transactions of the Institutions of Mining and Metallurgy

ISSN: 2572-6838 (Print) 2572-6846 (Online) Journal homepage: http://www.tandfonline.com/loi/yaes21

Heavy mineral resource potential of Tista river sands, Northern Bangladesh

P. K. Biswas, S. S. Ahmed, M. I. Pownceby, N. Haque, S. Alam, M. N. Zaman & M. A. Rahman

To cite this article: P. K. Biswas, S. S. Ahmed, M. I. Pownceby, N. Haque, S. Alam, M. N. Zaman & M. A. Rahman (2018): Heavy mineral resource potential of Tista river sands, Northern Bangladesh, Applied Earth Science, DOI: 10.1080/25726838.2018.1488357

To link to this article: https://doi.org/10.1080/25726838.2018.1488357

Published online: 22 Jun 2018.

Submit your article to this journal

View related articles

View Crossmark data

Full Terms & Conditions of access and use can be found at
http://www.tandfonline.com/action/journalInformation?journalCode=yaes21

APPLIED EARTH SCIENCE (TRANS. INST. MIN. METALL. B)
https://doi.org/10.1080/25726838.2018.1488357

The Institute of Materials, Minerals and Mining
AusIMM THE MINERALS INSTITUTE
Taylor & Francis
Taylor & Francis Group

Check for updates

Heavy mineral resource potential of Tista river sands, Northern Bangladesh

P. K. Biswas[a,b], S. S. Ahmed[b], M. I. Pownceby[c], N. Haque[c], S. Alam[a], M. N. Zaman[a] and M. A. Rahman[a]

[a]BCSIR Institute of Mining, Mineralogy and Metallurgy (IMMM), Khonjonpur, Bangladesh; [b]Department of Geology and Mining, University of Rajshahi, Rajshahi, Bangladesh; [c]CSIRO Mineral Resources, Clayton South, Australia

ABSTRACT

Surface and borehole sampling along a ~80 km section of the lower Tista river, northwestern Bangladesh, indicated that the river sands offer significant potential as a heavy mineral (HM) resource. Characterisation of sediments from the surface to 15 m depth showed that the sand-sized component was dominated by quartz, feldspar, mica, lithic fragments, amphibole and pyroxene group minerals. The most common particle size was between +125–500 µm with 84 wt-% of all material reporting to this size range. Laterally spaced sampling indicated slight grain size coarsening upstream. Heavy liquid separation studies revealed that HMs such as amphiboles, micas, garnets, aluminosilicate (Al2SiO5) phases, ilmenite and zircon made up ~10.99% (on average). The percentage of valuable HMs (ilmenite, rutile, zircon, monazite, garnet) was 2.47% (average). Detailed borehole sampling and resource mapping of a large, mid-channel sand bar showed that placer-style HM accumulations occur upstream and along the margins of the bar.

ARTICLE HISTORY
Received 26 April 2018
Accepted 7 June 2018

KEYWORDS
Tista river; heavy minerals; Rajpur mid-channel sand bar; HM resource maps

Introduction

Heavy minerals (HMs) are usually defined as those with a specific gravity >2.6 g cm^{-3} and include the highly sought-after element species gold and platinum. The majority of valuable heavy minerals (VHMs), however, occur as oxides and include economically important minerals rich in titanium, zirconium and rare earths (RE) as well as less VHMs including garnet, staurolite, sillimanite, etc. (Table 1). HMs typically occur in very low concentrations in a variety of igneous, metamorphic and sedimentary rock types and, being chemically and physically resistant to weathering, survive weathering and erosion of the host before being transported to low energy depositional sites. Economic concentrations of HMs are usually found in fluvial (e.g. sand bar) or beach shoreline (e.g. strandline) environments.

Bangladesh has known concentrations of HM sands along the southern and eastern coastlines associated with shoreline beach placer deposits (Mitra et al. 1992; Islam 1997; Kabir et al. 2006; Rajib et al. 2007). The identified HM suite of interest from these occurrences includes the minerals ilmenite, rutile, zircon and RE-containing monazite. Opportunities for developing HM deposits in Bangladesh have largely focused on the high-grade coastal sand deposits (Ahmed et al. 2010); however, recent work by Rahman et al. (2014, 2016) has explored the emerging potential for sourcing HMs from the widespread river sand bar placer deposits associated with some of the extensive sand-bedded river systems (e.g. the Brahmaputra-Jamuna and Ganges-Padma systems). These systems source sediments from a vast area extending across the tectonically active Himalayan Range (Garzanti et al. 2004) and represent a potentially large resource of VHMs.

River concentrations of HM are typically of low grade and usually comprise around 1–2% HMs, although several are higher grade (Zaman et al. 2012; Rahman et al. 2014). In comparison, beach or shoreline placer deposits can contain up to 23% total HM. Although of low grade, the latest estimated annual sediment load carried by the river systems in Bangladesh is about 2.4 billion tonnes highlighting the fact that these represent accumulations that are renewable.

The concentration of HM grains in sand-sized terrigenous sediments may fluctuate considerably because of several factors including provenance, sedimentary processes and post-depositional dissolution (Mange and Maurer 1992; Morton and Hallsworth 1999). Nonetheless, the chemical composition of mineral grains, their intergrowths with other minerals of similar size or with accessory minerals included in HM aggregates, may successfully be used to characterise the HM assemblage with respect to provenance and supergene alteration (Morton 1991; Dill 1998; Morton and Hallsworth 1999; Dill 2007).

This study has concentrated on the identification, description and abundance of the HM fraction in sediments sourced from the Tista river basin in northwestern Bangladesh, close to the border with India. The

CONTACT P. K. Biswas pradip_immm@yahoo.com BCSIR Institute of Mining, Mineralogy and Metallurgy (IMMM), Science Laboratory Road, Khonjonpur, Joypurhat 5900, Bangladesh; Department of Geology and Mining, University of Rajshahi, Rajshahi 6205, Bangladesh

© 2018 Institute of Materials, Minerals and Mining and The AusIMM

Table 1. Common economically important elements and minerals associated with HM placer-style deposits.

HM	Ideal formula	SG
Element species		
Gold	Au	15.6–19.3
Platinum	Pt	14–19
Diamond	C	3.5
Oxide species		
Ilmenite	$Fe^{2+}TiO_3$	4.7–4.8
Rutile	TiO_2	4.2–5.5
Anatase	TiO_2 – low T polymorph	3.8–4.0
Pseudorutile	$Fe_2^{3+}Ti_3O_9$	~3.8
Leucoxene	Alteration product of ilmenite	4.3–4.6
Zircon	$ZrSiO_4$	4.6–4.7
Monazite	$CePO_4$	5.0–5.3
'Spinel'	General name for mineral group with the formula - AB_2O_4 where A = Fe^{2+}, Mg) and B = (Cr^{3+}, Al^{3+})	3.5–5.2
Garnet	$Fe_3^{2+}Al_2Si_3O_{12}$ – almandine	3.5–4.3
Staurolite	$Fe_2^{2+}Al_9Si_4O_{23}(OH)$	3.7–3.8
Sillimanite	Al_2SiO_5 – high T polymorph	3.2–3.3
Kyanite	Al_2SiO_5 – high P polymorph	3.5–3.6
Corundum	Al_2O_3	4.0
Quartz	SiO_2	2.6–2.7
Titanite	$CaTiSiO_5$	3.45–3.55
Cassiterite	SnO_2	6.8–7.0
Wolframite	$(Fe,Mn)WO_4$	7.1–7.5

geomorphic, depositional environment, provenance and hydrologic characteristics of the Tista fan located in Bangladesh has previously been extensively studied (Chakraborty and Ghosh 2010; Ghosh 2015; Khan and Islam 2015), while the Siwalic sediments of the Indian section of the Tista river valley was studied by Kundu et al. (2012). Mineralogical studies of sediments based on the surface sampling data (Garzanti et al. 2004; Rahman et al. 2014; Vezzoli et al. 2017) demonstrated quartz, feldspar and low-rank metamorphic lithic grains formed the major light mineral component, whereas the HM suite comprised amphiboles, garnet and sillimanite with minor opaques (magnetite, ilmenite, rutile). A previous economic analysis of Tista-derived sediments by Hossain et al. (2013) was limited to an evaluation of the potential for producing glass sand; while more recently, Rahman et al. (2017) conducted a preliminary analysis of the economic viability of the sands through a consideration of all potentially recoverable components. In this current study, the focus was on characterising the distribution, mineralogy and abundance of the more VHM components of the Tista river sediments, in particular, the minerals ilmenite, rutile, zircon, monazite and garnet. Results provide a starting point for the possible development of Tista river sediments as a potentially renewable resource of VHMs.

Study area and sampling

The Tista river is a tributary of the Jamuna river system which flows through India and northern Bangladesh. It flows in a southeast direction for a distance of approximately 309 km from its source region ~7000 m above sea level in the Himalayan Pahunuri glacier in the North Sikkim region (India) (Mukhopadhyay 1982) where it drains tectonic units of diverse geology (Gansser 1964; Vezzoli et al. 2017). The Tista river is fed by tributaries arising in the Thangu, Yumthang and Donkia-La Ranges and is met by its main tributary, the Rangeet river at Triveni, India. The Tista river enters Bangladesh at the Kharibari border, Nilphamari district, whereupon it flows ~124 km in a southeasterly direction crossing the Rangpur region of Bangladesh to eventually merge with the Jamuna River near Chilmari.

Within Bangladesh, the bed profile of the Tista river changes from a sand-dominated bed of approximately 10 m depth in the northwestern segment near the Tista barrage (26°45′13″N; 88°35′22″E) to a bed profile made up of approximately 20 m of gravel in the most southerly section near the Tista bridge. Extensive mid-channel sand bars, known locally as *chars*, develop in the central parts of the river and these are elongated in an NW-SE direction. The width of the most recently developed sand bars ranges from ~200 to 500 m and the lengths are typically between 700 and 1500 m.

During fieldwork conducted on the riverbanks and chars, bulk surface and bore samples were collected extending from the surface to ~17 m depth (using tube well boring). In the first phase of sampling, 18 surface samples (labelled ST) and three tube-well wash bore samples (labelled BST) with depths of up to 17 m were collected laterally along ~80 km of the Tista river (Figure 1(A)). In the second phase of sampling, material was collected from a longitudinal mid-channel sand bar (~8 km^2 in area) at Rajpur (Figure 1(B)). The material sampled included 45 pit (0–1.5 m depth) samples collected using a square grid pattern using a 500 m station spacing (denoted as sites A–E, 1–9) and eight tube-well wash bore samples spaced ~1 km apart and with samples collected to a depth of up to 1 m. For sampling the pit samples, the whole wall section was scraped to a depth of ~50 cm. Duplicate samples were collected on ~20% of samples with the frequency determined on the basis of field observations.

Materials and methods

Grain size analysis

In the laboratory, the samples were treated with 1N HCl and washed with distilled water to remove carbonate particles. The sand was then oven-dried overnight at 110°C and 100 g of each sample was sieved for 15 min using a Retsch vibratory sieve shaker to determine the distribution of particles in the following size intervals: >2 mm; −2 + 1 mm; −1 + 0.5 mm; −500 + 250 µm; −250 + 125 µm; −125 + 63 µm; −63 + 45 µm and −45 µm.

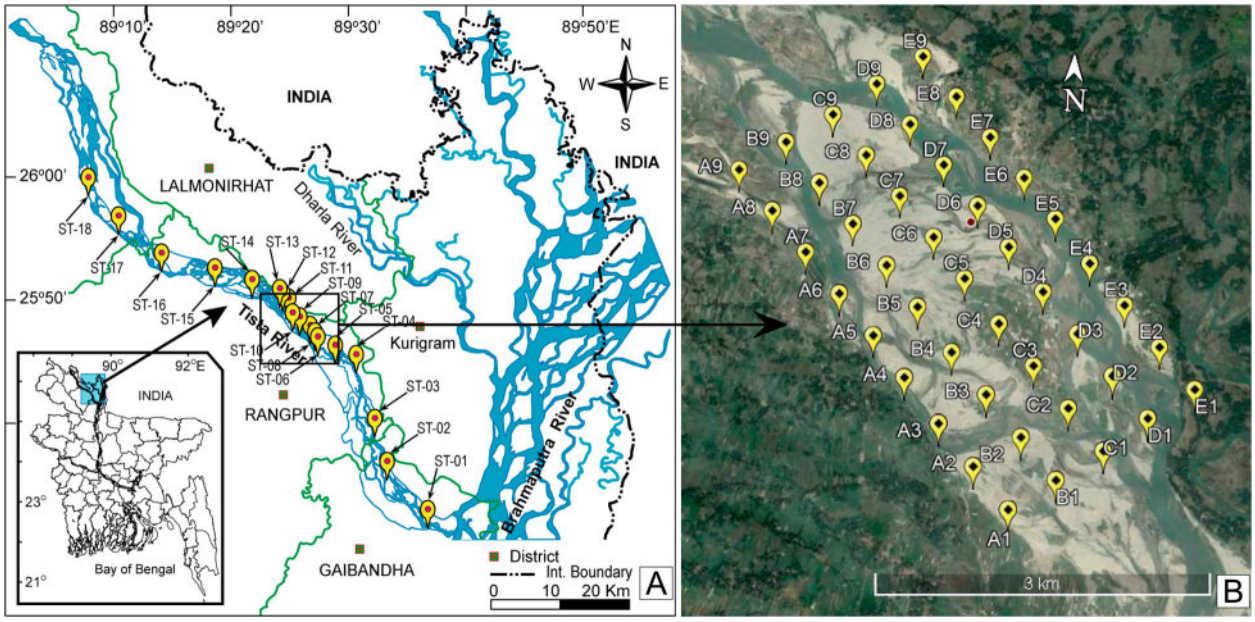

Figure 1. Location map showing the study area (A) along the Tista river and (B) a satellite image of the sand bar extensively sampled in Rajpur region of the Tista river (after Zaman et al. 2012).

Heavy liquid separation

HM analysis was performed on the very fine to medium size sand fraction (−500 + 63 μm) from more than 200 samples sampled at different depths (e.g. surface to 17 m). The HMs were separated by gravity settling using tetrabromoethane of specific gravity ~2.96 g cm^{-3}. For each test, 10 g of washed sample was used with occasional stirring (up to three times per test). Settling times were on the order of 45 min to 1 h.

Mineralogical analysis

A total of 69 samples were analysed in the mineralogical study: two bulk samples (labelled Bulk 1 Raw and Bulk 2 Raw); 18 laterally spaced surface samples (ST01–ST18); 3 well bore samples from ~80 km along the Tista river (BST-02; BST-10 and BST-18); 45 pit samples and 1 tube well sample (TBC-6) from the Rajpur mid-channel sand bar. The two bulk samples were composite samples from regions along the river bank where there was a visible natural concentration of HMs (as indicated by a higher proportion of dark minerals). The two bulk samples and the two pit samples (D4 and B7) were further processed using a shaking table to remove light minerals and to concentrate the HMs.

Two thin sections were prepared for each sample. The mineralogical studies were carried out using a MEIJI ML 9000 polarising and a MEIJI EMZ-5TR stereo microscope. The HMs including opaques (ilmenite, rutile, etc.) and non-opaque's (zircon, kyanite, etc.) were point counted along 10–15 suitably spaced traverses. The HM components were estimated by counting a minimum of 200 grains by the ribbon method as described in Mange and Maurer (1992). The colour, crystal habit, size and other characteristics of the minerals were also observed and noted. Photomicrographs were taken by using a COOLPIX camera attachment.

X-ray diffraction

Each sample (5 g) was micronised in ethanol using a McCrone micronizer (4 min g^{-1}), centrifuged and dried at 60°C before gentle hand mixing in a mortar and pestle to break up any agglomerates and to ensure homogeneity. Samples were either back-pressed into PANalytical sample holders or front-pressed onto low-background plates, depending on the quantity of sample, for flat plate presentation to the X-ray beam. Diffraction data were collected from 5° to 140° 2θ using a PANalytical MPD instrument fitted with a cobalt long-fine-focus X-ray tube operated at 40 kV and 40 mA. The incident beam path was defined using 0.04 radian Soller slits, and a 0.5° fixed divergence slit. The diffracted beam incorporated a graphite monochromator to eliminate unwanted wavelengths and a 4.6 mm anti-scatter slit. An X'Celerator detector was used in scanning line (1D) mode with an active length of 2.122° 2θ. Data were collected with a nominal step size of 0.033° 2θ (~4 h per scan). Samples were rotated at 60 rpm during data collection to improve particle statistics.

Phase identification was performed using PANalytical Highscore Plus© software (Degen et al. 2014) which interfaces with the PDF4+ database (ICDD 2016). Quantitative phase analysis (QPA) was carried out

via the Rietveld method (Rietveld 1969; Hill and Howard 1987) using TOPAS V5 software (Bruker AXS 2013).

Results

Grain size analysis

The average grain size distributions measured for the 70 samples are shown in Figure 2(A). For the surface samples (depth to ~1 m) sourced from laterally along the river (ST01–ST18), the most common particle size was between +125 and 500 µm with 84 wt-% of all material reporting to the size range (i.e. 30 wt-% to the +250 to 500 µm fraction and 53 wt-% to the +125 to 250 µm fraction). These are classified as medium- to coarse-grained sands (Blott and Pye 2012). The analysis data from the three well bores BST-02; BST-10 and BST-18 is slightly skewed towards the coarser grain size fractions suggesting an overall increase in coarse sand grain size at depth. A comparison with the tube well data from the Rajpur mid-channel sand bar (TBC-6) also indicates a coarse sand grain size with 54 wt-% of material reporting to the +250 to 500 µm fraction.

To examine the variation in grain size laterally along the river, grain size analysis results from the +125 to 250 µm and +500 µm to 1 mm fraction of the ST01 to ST18 samples are plotted in Figure 2(B). Sample ST-01 is located furthest downstream, close to the confluence of the Tista river with the Jamuna river and sample ST-18 is upstream. The results show that the upstream component of the sand is characterised by a higher proportion of coarser particles, whereas finer particles increase downstream (Figure 2(B)).

Heavy liquid separation

Heavy liquid separation studies were conducted on the +63 to 500 µm size fractions prepared from the 45 samples from the Rajpur longitudinal mid-channel sand bar, 18 lateral samples along the Tista river and also from 3 bore wells from the laterally spaced sample sites.

Rajpur longitudinal sand bar

The location of individual sample sites from the Rajpur longitudinal sand bar is shown in Figure 1(B) and wt-% data for the distribution of light and heavy components of the sand fraction from the interval surface to 1.5 m depth are provided in Table 2. The concentration of HMs varies from 4.6% (sample site B-03) to 14.9% (A-04) and light minerals from 84.1% (A-4) to 93.9%

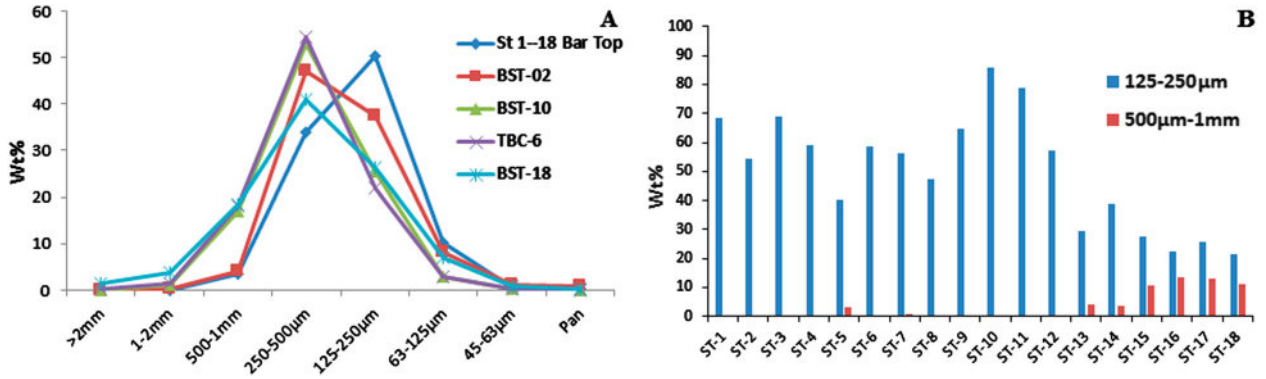

Figure 2. (A) Average grain size distribution of selected bulk samples from the Tista river. (B) The average size distributions (+125 to 250 µm and +500 µm to 1 mm).

Table 2. Heavy (H%) and light (L%) mineral distributions in 45 bulk samples (+63 to 500 µm fraction) collected from the Rajpur mid-channel sand bar (all data in wt-%).

	+63 to 500 µm size fraction									
Line No	A		B		C		D		E	
	H%	L%	H%	L%	H%	L%	H%	L%	H%	L%
01	6.4	92.8	9.2	89.3	8.1	91.6	5.2	93.9	13.6	86.1
02	13.8	85.3	11.5	87.2	9.5	89.2	10.9	89.6	11.6	87.4
03	11.1	87.8	4.6	90.4	11.3	87.7	7.9	91.7	10.8	88.7
04	14.9	84.1	10.7	88.6	8.6	89.9	11.2	88.0	12.3	86.1
05	11.8	86.6	10.0	89.5	8.4	88.5	7.7	91.0	11.6	87.9
06	12.8	86.7	10.9	88.7	11.2	88.4	12.0	87.1	12.7	86.9
07	11.6	88.2	13.8	85.8	9.3	89.6	10.5	88	6.8	92.6
08	11.9	87.7	11.9	86.8	13.6	86.1	9.6	89.6	13	85.4
09	13.0	86.9	12.5	86.8	11.8	86.7	8.1	90.5	11.1	87.8
Avg.	11.9	87.3	10.6	88.1	10.2	88.6	9.1	89.9	11.5	87.7

(D-1). The average heavy and light mineral percentages across all sites were 10.7% and 88.3%, respectively.

Laterally spaced samples

The concentration of HMs in the bulk samples ST01 to ST18 sampled along the Tista river varies from 9.3% (ST-15) to 15.2% (ST-03) with an average 11.8%. The light mineral component dominates and varies from 84.8% to 90.7% with an average content of 88.2% (Table 3).

Table 3. The heavy (H%) and light (L%) minerals distribution in the laterally spaced bulk samples (+63 to 500 µm fraction) (all data in wt-%).

Sample	H%	L%	Sample	H%	L%
ST-01	9.9	90.1	ST-10	11.4	88.6
ST-02	12.5	87.5	ST-11	12.2	87.8
ST-03	15.2	84.8	ST-12	10.7	89.3
ST-04	12.1	87.9	ST-13	13.2	86.8
ST-05	10.4	89.6	ST-14	12.6	87.4
ST-06	12.2	87.8	ST-15	9.3	90.7
ST-07	9.5	90.5	ST-16	9.8	90.2
ST-08	12.6	87.4	ST-17	11.6	88.4
ST-09	12.8	87.2	ST-18	14.1	85.9

Borehole samples

The average concentration of HMs in the laterally spaced bores BST-02, BST-10 and BST-18 was 8%, 11% and 15%, respectively (Figure 3). In this figure, the individual borehole data of up to 17 m in depth is compared with the average data for the bulk surface samples (ST01 to ST-18). As previously stated, the average HM content for the bulk surface samples was 11.8%. In comparison, the data for the boreholes show considerable variation with depth and individual boreholes reveal a systematic variation in HM concentration with BST-18 (upstream) comprising a greater amount of HMs compared to BST-02 which is further downstream.

Detailed data for the size fractions +63 to 125, +125 to 250 and+250 to 500 µm and the corresponding per cent HMs results versus depth for one of the boreholes (BST-02) is provided in Table 4. Also included is the average data for the size interval +63 to 500 µm based on a composite sample generated by combining all three size fractions (last two columns). Overall, the sample contained on average, 8.1% HM, however, there

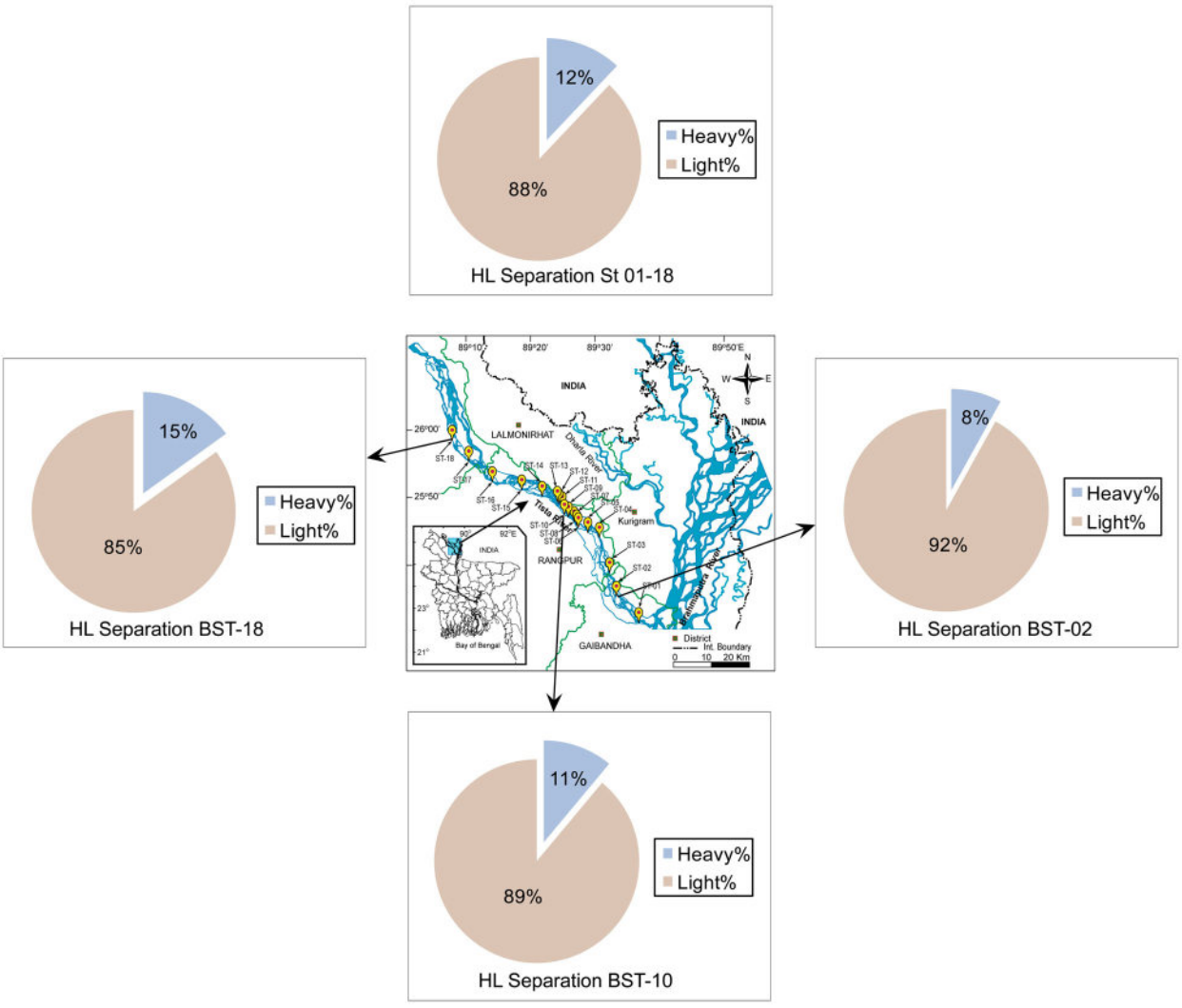

Figure 3. Comparison of the abundance of heavy and light minerals in the selected borehole samples (BST-02, BST-10 and BST-18) and the average content in the surface samples ST01–ST18.

Table 4. Size and heavy (H%) and light (L%) minerals distributions with depth for borehole sample BST-02 (all data in wt-%).

		+63 to 125 µm		+125 to 250 µm		+250 to 500 µm		+63 to 500 µm	
Sample	Depth(m)	H%	L%	H%	L%	H%	L%	H%	L%
1	0–0.91	12.30	87.30	16.24	83.758	15.21	81.79	12.5	87.5
2	0.9–1.8	11.60	88.20	8.08	91.916	11.62	88.38	8.5	91.2
3	1.8–2.7	18.67	84.33	5.57	94.434	6.12	93.88	6.4	93
4	2.7–3.6	5.26	94.74	7.66	92.337	5.59	94.41	6.5	92.5
5	3.6–4.5	5.00	95.00	10.89	89.11	8.47	91.53	8.6	91.2
6	4.5–5.4	4.48	95.52	7.32	92.68	9.02	90.99	8.9	90.7
7	5.4–6.4	12.77	80.85	8.37	91.64	7.68	92.33	9.1	90.3
8	6.4–7.3	7.69	92.31	6.83	93.17	8.59	91.41	6	80.3
9	7.3–8.2	8.89	91.11	8.75	91.25	7.93	92.07	8.6	90.6
10	8.2–9.1	9.77	89.55	9.81	90.19	6.79	93.21	7.3	92.4
11	9.1–10.0	10.44	88.96	6.27	93.73	6.60	93.40	7.6	91.7
12	10.0–10.9	12.92	86.24	8.14	91.86	8.83	91.17	7.7	90.8
Average		9.98	89.51	8.66	91.34	8.54	91.21	8.14	90.18

Table 5. The heavy (H%) and light (L%) minerals distribution with depth for the −500+63 µm size fraction for the bore samples TBC-6, BST-10 and BST-18 (all data in wt-%).

		TBC-6		BST-10		BST-18	
Sample	Depth(m)	H%	L%	H%	L%	H%	L%
1	0–0.91	9.2	90.2	8.1	91.9	10.1	89.9
2	0.9–1.8	10.6	88.1	10.0	90.0	21.3	78.7
3	1.8–2.7	11.8	87.7	10.3	89.68	–	–
4	2.7–3.6	13.6	85.8	13.9	86.12	13.4	86.6
5	3.6–4.5	7.7	91.2	16.5	83.55	13.1	86.9
6	4.5–5.4	9.9	89.9	14.0	86.0	10.2	89.8
7	5.4–6.4	11.6	87.6	9.0	91.0	17.1	82.9
8	6.4–7.3	8.4	91.8	9.6	90.4	17.4	82.6
9	7.3–8.2	7.8	92	12.4	87.6	11.8	88.2
10	8.2–9.1	7.2	92.7	10.1	89.9	17.3	82.7
11	9.1–10.0	8.3	91.2	9.4	90.6		
12	10.0–10.9	11.3	88.5	9.4	90.6		
13	10.9–11.8	9.6	89.8	10.1	89.9		
14	11.8–12.8	10.2	89.8	9.0	91.0		
15	12.8–13.7	10.3	89.3				
16	13.7–14.6	9.1	90.2				

was considerable variation in HM content with both depth and grain size. For all size fractions examined, the upper 2–3 m had the greatest concentration of HMs, while the finer +63 to 125 µm size fraction had the highest average HM content (column 3 at 9.98% HM). For the remaining boreholes BST-10 and BST-18, data for the +63 to 500 µm fraction provided in Table 5 indicate the HMs are concentrated in the upper layers although since these boreholes are located further upstream than BST-02, the overall abundance of HMs is generally greater at all depths. Moreover, in the furthest upstream sample (BST-18), the HM content is up to 21.3% of the total light + heavy sediment load consistent with the previously noted increase in total HM content further upstream. Table 5 also includes detailed size and total HM content results for tube test well TBC-6 taken from the mid-channel sand bar (location C6, Figure 1(B)). Results suggest a relatively constant concentration of HMs with depth, varying between 7.2 and 13.6 wt-% HM.

Mineralogy

HM assemblage by X-ray diffraction. To assess the mineralogy of the HMs found in the Tista river sands, two bulk samples (Bulk Raw 1 and Bulk Raw 2) and two pit samples (D4 and B7) from the Rajpur mid-channel sand bar were examined using X-ray diffraction (XRD). The Bulk Raw 1, Bulk Raw 2 and D4 and B7 samples were then further processed using a shaking table to remove light minerals and to concentrate the HMs. The results of the phase identification and QPA by XRD are given in Table 6. The QPA results are relative weight percentages and do not include any unidentified or amorphous material which may exist in the samples.

Although naturally concentrated in HMs, the unprocessed bulk sand samples were still dominated by a high-quartz content (>45 wt-% in Bulk Raw 1) with additional large amounts of 'light' aluminosilicate minerals including feldspars, micas and minor amounts of chlorite. The detailed phase analysis identified individual feldspar subtypes including both albite and anorthite feldspar; however, while end-member structure types for these phases were used to quantify the amount of each of these minerals, their compositions are yet to be verified (e.g. by energy dispersive X-ray analysis or by electron probe microanalysis). For this reason, the phase assemblage is reported as mineral groups rather than individual mineral phase types. HMs make up ~25% of the bulk sand samples and are composed primarily of amphiboles, garnets, pyroxenes and aluminosilicate (Al_2SiO_5) phases. Ilmenite was present at levels of ~2% while other economically important HM's such as zircon and rutile were close to or below, the detection limit of XRD (i.e. <~1%).

Processing of the two bulk sand samples as well as the D4 and B7 pit samples to remove a large proportion of the light minerals quartz and feldspar, resulted in an increase in the amount of HMs recovered and a significant change in the overall mineral assemblage. Heavier minerals such as amphiboles (including the subtypes hornblende and actinolite) increased in abundance along with garnet and pyroxenes. The ilmenite content was also significantly upgraded (by at least a factor of two) and other VHMs such as zircon and rutile were identifiable in small amounts.

Table 6. Quantitative X-ray diffraction results from the Raw Bulk 1 sample and shaking table concentrates produced from samples: Bulk 1 Raw, Bulk 2 Raw and pit samples D4 and B7 from the Rajpur mid-channel sand bar (all data in relative wt-%, n.d. = not detected).

Sample	Quartz	Ilmenite	Chlorite	Amphibole Group	Feldspar Group	Mica Group	Pyroxene Group	Apatite	Garnet Group	Al_2SiO_5 Group	Zircon	Rutile
Bulk 1 Raw	45.3	1.9	2.2	5.6	16.8	10.6	n.d.	n.d.	14.1	3.0	n.d.	n.d.
Bulk 1 Shaking Heavy	22.3	3.5	1.8	10.6	7.7	5.1	5.8	1.5	36.2	3.9	n.d.	0.9
Bulk 2 Shaking Heavy	18.1	2.6	1.4	12	5.4	4.2	6.6	2.5	42.9	2.6	n.d.	1.0
D-4 Pit Shaking Heavy	16.1	8.3	2.3	14.2	1.5	4.0	4.7	4.2	40.6	n.d.	1.7	1.8
B-7 Pit Shaking Heavy	20.2	5.5	2.6	11.3	5	2.3	4.7	3.5	38.9	2.9	1.0	1.4

Table 7. HMs determined using optical microscopy in the bulk surface samples ST01–ST18 (0–1 m).

Mineral	ST-01	ST-02	ST-03	ST-04	ST-05	ST-06	ST-07	ST-08	ST-09	ST-10	ST-11	ST-12	ST-13	ST-14	ST-15	ST-16	ST-17	ST-18	Average
Magnetite	0.0	0.1	0.1	0.1	0.1	0.1	0.0	0.1	0.1	0.1	0.1	0.1	0.1	0.1	0.0	0.0	0.1	0.1	0.1
Ilmenite	0.3	0.5	0.7	0.5	0.3	0.5	0.4	0.5	0.7	0.4	0.5	0.4	0.7	0.5	0.4	0.5	0.3	0.5	0.5
Rutile	0.0	0.1	0.2	0.2	0.0	0.2	0.1	0.2	0.2	0.1	0.2	0.1	0.3	0.2	0.1	0.1	0.1	0.1	0.1
Zircon	0.0	0.1	0.1	0.2	0.1	0.1	0.1	0.1	0.1	0.1	0.1	0.1	0.1	0.1	0.1	0.1	0.2	0.1	0.1
Garnet	0.2	0.4	2.6	1.1	0.3	1.9	0.5	1.6	2.2	0.5	0.7	0.6	1.9	1.9	1.2	1.4	1.3	1.3	1.2
Monazite	0.0	0.1	0.1	0.1	0.0	0.1	0.1	0.1	0.1	0.1	0.1	0.1	0.1	0.1	0.1	0.1	0.1	0.1	0.1
Kyanite	0.1	0.1	0.2	0.1	0.1	0.1	0.1	0.3	0.1	0.1	0.1	0.1	0.2	0.1	0.1	0.1	0.1	0.2	0.1
Sillimanite	0.1	0.1	0.2	0.1	0.1	0.1	0.0	0.1	0.1	0.1	0.1	0.1	0.1	0.1	0.1	0.0	0.1	0.1	0.1
Mica	6.5	7.7	7.3	6.5	6.5	5.9	5.8	6.7	6.1	6.8	7.2	6.2	6.4	6.5	4.9	4.8	6.0	7.5	6.4
Others	2.7	3.4	3.9	3.4	3.1	3.3	2.5	3.0	3.1	3.2	3.2	3.0	3.4	3.0	2.3	2.7	3.4	4.2	3.1
VHMC	0.7	1.4	4.1	2.2	0.8	3.0	1.2	2.9	3.6	1.4	1.8	1.5	3.4	3.1	2.1	2.3	2.2	2.4	2.2

Note: 'Others' refers to lithic fragments while the term VHMC (last row) refers to the aggregate of the valuable heavy mineral components; ilmenite, rutile, zircon, garnet, monazite, kyanite and sillimanite.

Optical microscopy

To examine whether the mineral content was consistent throughout the area studied, the HMs present in the laterally spaced samples and the borehole samples were identified and their abundances determined via point counting using both polarising and stereo microscopes. The weight percentage of the individual mineral types identified were calculated by multiplying the modal point count result with the specific gravity for each mineral.

Laterally spaced samples. The types and abundances of HMs identified in the 18 laterally spaced surface samples (0–1 m) are summarised in Table 7. For all samples, the HM component was dominated by garnet and ilmenite followed by zircon, rutile, kyanite, sillimanite and magnetite in lesser amounts. Approximately 10% of the heavy fraction consisted of micas (muscovite and/or biotite) and undifferentiated lithic fragments.

Borehole samples. Data for the HM content versus depth for the borehole samples BST-02, BST-10 and BST-18 are shown in Tables 8–10, respectively. Representative stereo and polarised light photomicrographs from each of these samples are provided in Figure 4. The tabulated data show that the average HM content was lowest in BST-02 (downstream) and highest in BST-18 (upstream). There was no observable trend with depth with the exception being BST-18 where the highest HM concentrations occurred in the interval 5.4–9.1 m. In all samples, the valuable heavy mineral component (VHMC) was characterised by (in order of abundance) garnet and ilmenite. Minor VHMC phases included magnetite, rutile, zircon, monazite, kyanite and sillimanite. Gangue phases present were micaceous phases (muscovite and biotite) and unidentified phases, predominantly made up of lithic fragments.

Point count data was also collected for the tube test well sample TBC-6 (mid-channel sand bar, location C6, Figure 5). The concentration of the VHMs varied with the depth of up to 15 m similar to other borehole samples. Average VHMC data for the TBC-6 core was: 0.05% magnetite; 0.40% ilmenite; 0.09% rutile; 0.13%

Table 8. Weight percentage of HMs with depth in borehole BST-02.

Depth (m)	0–0.91	0.9–1.8	1.8–2.7	2.7–3.6	3.6–4.5	4.5–5.4	5.4–6.4	6.4–7.3	7.3–8.2	8.2–9.1	9.1–10.0	10.0–10.9	Avg
Magnetite	0.08	0.08	0.03	0.04	0.05	0.04	0.04	0.03	0.04	0.05	0.03	0.04	0.05
Ilmenite	0.61	0.30	0.21	0.40	0.64	0.54	0.49	0.31	0.33	0.29	0.28	0.59	0.41
Rutile	0.22	0.22	0.07	0.20	0.21	0.19	0.22	0.14	0.18	0.19	0.17	0.16	0.18
Zircon	0.24	0.06	0.12	0.17	0.16	0.21	0.18	0.10	0.13	0.14	0.09	0.11	0.14
Garnet	0.62	0.52	0.43	0.77	1.23	0.64	0.78	0.52	0.56	1.36	0.71	1.25	0.78
Monazite	0.25	0.12	0.09	0.17	0.25	0.16	0.25	0.10	0.13	0.15	0.14	0.18	0.17
Kyanite	0.27	0.18	0.12	0.13	0.30	0.20	0.50	0.23	0.25	0.22	0.17	0.31	0.24
Sillimanite	0.17	0.08	0.06	0.08	0.16	0.07	0.12	0.07	0.09	0.10	0.06	0.12	0.10
Mica	9.02	4.31	2.92	3.77	5.34	3.57	3.99	3.66	4.72	4.76	3.03	3.48	4.38
Others	4.51	2.21	1.52	1.95	2.56	1.71	1.79	1.67	2.32	2.55	1.59	1.91	2.19
VHMC	2.45	1.56	1.13	1.95	3.00	2.05	2.58	1.50	1.71	2.50	1.65	2.75	2.07

Table 9. The weight percentage of HMs with depth in borehole BST-10.

Depth (m)	0–0.91	0.9–1.8	1.8–2.7	2.7–3.6	3.6–4.5	4.5-5.4	5.4–6.4	6.4–7.3	7.3–8.2	8.2–9.1	9.1–10.0	10.0–10.9	10.9–11.8	11.8–12.8	Avg
Magnetite	0.04	0.05	0.05	0.07	0.08	0.07	0.05	0.05	0.06	0.05	0.05	0.05	0.05	0.05	0.05
Ilmenite	0.30	0.37	0.46	0.61	0.84	0.52	0.47	0.56	0.72	0.53	0.35	0.35	0.45	0.27	0.49
Rutile	0.16	0.27	0.28	0.36	0.43	0.19	0.12	0.13	0.16	0.13	0.12	0.13	0.13	0.06	0.19
Zircon	0.12	0.15	0.08	0.10	0.12	0.10	0.07	0.07	0.18	0.07	0.07	0.14	0.07	0.07	0.10
Garnet	0.82	1.02	1.11	2.34	2.56	2.04	0.69	1.50	2.15	1.28	1.37	1.31	1.47	0.70	1.45
Monazite	0.12	0.08	0.08	0.10	0.25	0.11	0.14	0.07	0.18	0.08	0.14	0.07	0.08	0.07	0.11
Kyanite	0.14	0.22	0.23	0.38	0.36	0.31	0.20	0.16	0.20	0.11	0.16	0.10	0.11	0.05	0.19
Sillimanite	0.04	0.10	0.05	0.07	0.16	0.21	0.09	0.05	0.06	0.05	0.05	0.05	0.10	0.09	0.08
Mica	3.92	5.07	5.23	6.47	7.65	7.00	4.80	4.55	5.57	5.11	4.61	4.62	4.86	4.87	5.31
Others	2.43	2.67	2.75	3.38	4.00	3.45	2.37	2.42	3.11	2.69	2.49	2.59	2.78	2.76	2.85
VHMC	1.75	2.26	2.34	4.03	4.80	3.54	1.83	2.58	3.72	2.31	2.30	2.19	2.47	1.36	2.68

Table 10. The weight percentage of HMs with depth in borehole BST-18.

Depth (m)	0–0.91	0.9–1.8	2.7–3.6	3.6–4.5	4.5–5.4	5.4–6.4	6.4–7.3	7.3–8.2	8.2–9.1	Average
Magnetite	0.10	0.11	0.07	0.13	0.10	0.17	0.17	0.12	0.17	0.13
Ilmenite	0.31	0.17	0.70	0.49	0.61	1.00	0.65	0.44	0.51	0.54
Rutile	0.07	0.00	0.18	0.18	0.14	0.34	0.35	0.23	0.34	0.20
Zircon	0.00	0.00	0.10	0.10	0.07	0.12	0.00	0.09	0.12	0.07
Garnet	0.46	0.43	1.70	1.26	0.97	2.67	2.21	1.63	2.92	1.58
Monazite	0.08	0.00	0.10	0.10	0.08	0.00	0.00	0.09	0.13	0.06
Kyanite	0.06	0.13	0.15	0.07	0.11	0.19	0.10	0.19	0.28	0.14
Sillimanite	0.05	0.00	0.07	0.07	0.10	0.17	0.09	0.06	0.17	0.09
Mica	6.09	14.45	6.77	7.24	5.39	8.12	8.98	5.38	7.53	7.77
Others	2.88	6.02	3.57	3.46	2.62	4.32	4.81	3.56	5.11	4.04
VHMC	1.13	0.83	3.06	2.40	2.19	4.66	3.57	2.85	4.66	2.82

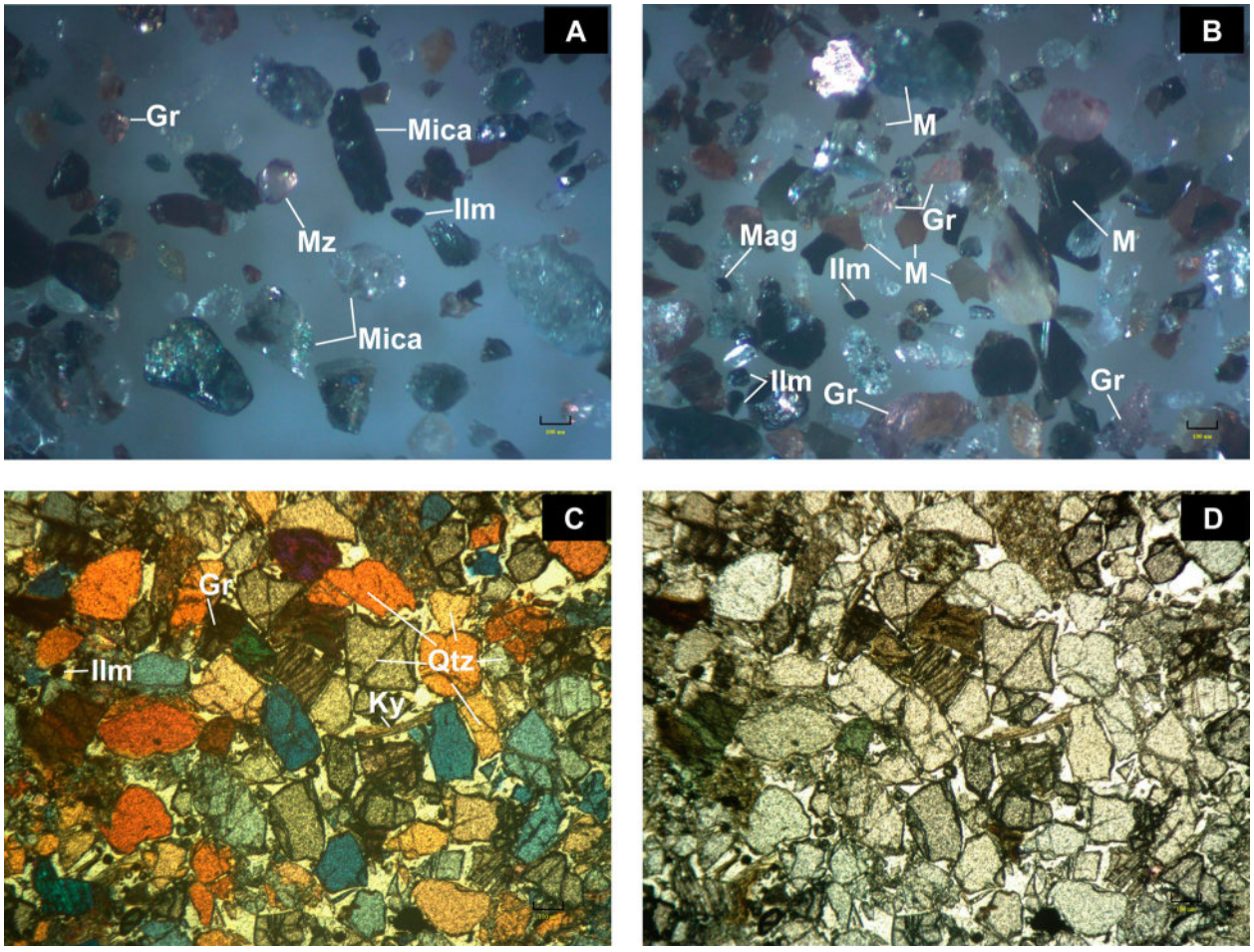

Figure 4. Photomicrographs showing: (A) BST-10 heavy mineral fraction, stereomicroscope image 4.5× mag., (B) BST-18 heavy mineral fraction, stereomicroscope image 4.5× mag., (C) ST-03 bulk sample image, crossed nicols 4.0× mag., (D) same view of ST-03 bulk sample as shown in (C) but under plane polarised light, 4.0× mag. (Ilm-ilmenite, Gr-garnet, M-mica, Mz-monazite, Qtz-quartz, Ky-kyanite, Mag-magnetite).

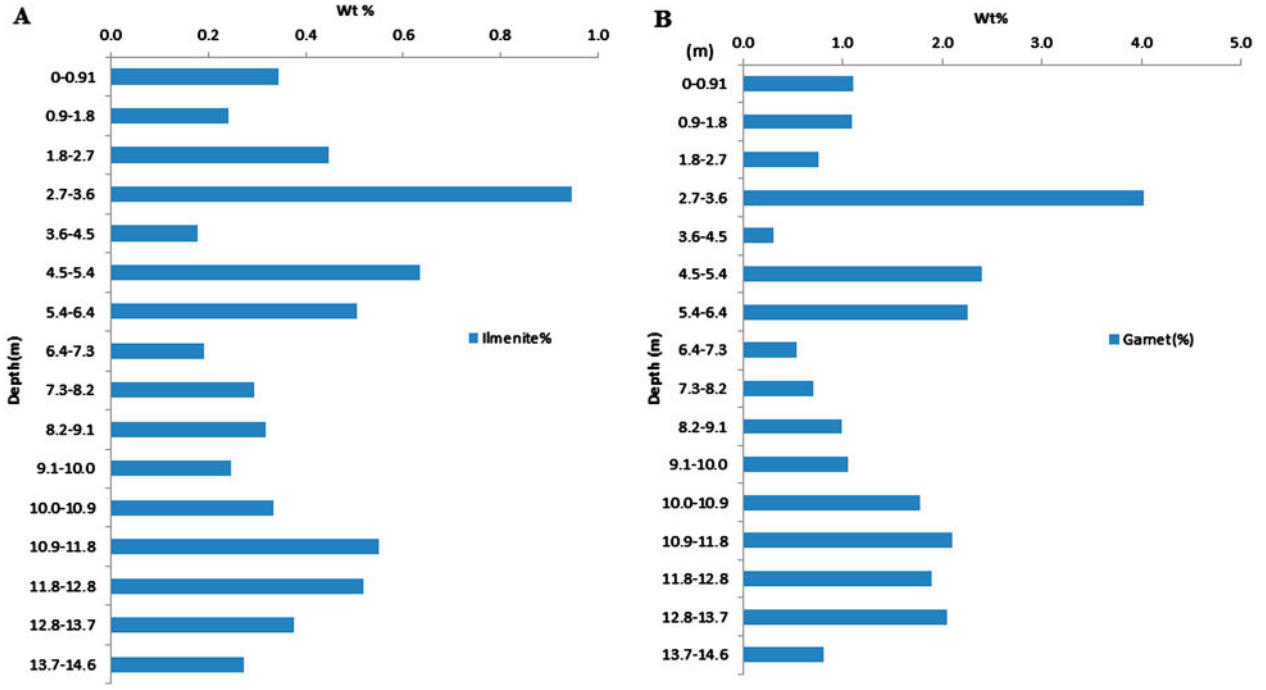

Figure 5. Concentration of ilmenite (A) and garnet (B) with depth in tube bore sample TBC-6 from the Rajpur mid-channel sand bar.

zircon; 1.49% garnet; 0.10% monazite; 0.14% kyanite and 0.09% sillimanite.

Rajpur mid-channel sand bar. Quantitative point count analysis was conducted on all 45 samples from the Rajpur mid-channel sand bar. Average data across all sites from each of the line sections A through E are provided in Table 11. The sands of the Rajpur bar show an average VHMC of >3% along lines A and B closest to the southwest bar margin (e.g. lines A2, B2, A4, B4, A7, B7, A9 and B9) and also along line E of the north-east bar margin. In comparison, for lines C and D towards the central region of the bar, the average VHMC is comparatively lower (1.81% and 2.04%, respectively). The highest VHMC concentration occurred at sample site B7, close to the bar head, while the lowest concentration was at sample site D1, the distal end of the bar.

Table 11. HM distribution of the Tista river, Rajpur mid-channel sand bar.

	Line					
Minerals	A	B	C	D	E	Avg
Magnetite	0.06	0.05	0.05	0.05	0.06	0.05
Ilmenite	0.53	0.57	0.44	0.47	0.48	0.50
Rutile	0.10	0.11	0.06	0.09	0.09	0.09
Zircon	0.22	0.19	0.11	0.19	0.21	0.18
Garnet	1.75	1.57	0.85	0.91	1.51	1.32
Monazite	0.13	0.15	0.09	0.10	0.11	0.12
Kyanite	0.14	0.16	0.15	0.14	0.12	0.14
Sillimanite	0.14	0.14	0.07	0.10	0.13	0.12
Mica	4.48	3.94	3.56	3.75	4.88	4.12
Dark minerals	4.37	3.44	3.27	3.34	3.91	3.67
VHM	3.06	2.94	1.81	2.04	2.71	2.51

Resource mapping and economic potential of the Tista river sands

Sand and gravel are the most-extracted materials in the world, exceeding fossil fuels and biomass (measured by weight). Sand is a key ingredient for concrete, roads, glass and electronics and massive amounts of sand are mined for land reclamation projects, shale gas extraction and beach re-nourishment programmes. Bangladesh currently mines extensive amounts of sand from its river systems and alluvial plains (Chowdhury et al. 2014; Hossain et al. 2013) through dredging operations. These operations are mainly aimed at removal of sediment and other material for the purpose of deepening rivers and ports to make waterways navigable, to obtain fill material or for the formation of levees to prevent flooding. Sand is an existing by-product of these operations; however, there are opportunities to boost the economics of sand processing and general waterway dredging operations through the by-product recovery of the VHMCs of the existing sand resources. To recover the VHMCs from dredging operations a floating dredge would cut and suction the ore-containing sediment under the surface and pump the slurry to a wet concentrator floating behind the dredge. The floating concentrator would contain screens to remove the oversize fraction (typically >150 to 250 mm), hydrocyclones to remove fine-grained clays and banks of spiral gravity separators to produce an initial HMC. The HMC would then be processed onshore using standard dry processing separation procedures involving a combination of gravity, magnetic/electrostatic separation circuits to separate the valuable minerals from the non-valuable minerals to make the ilmenite, rutile

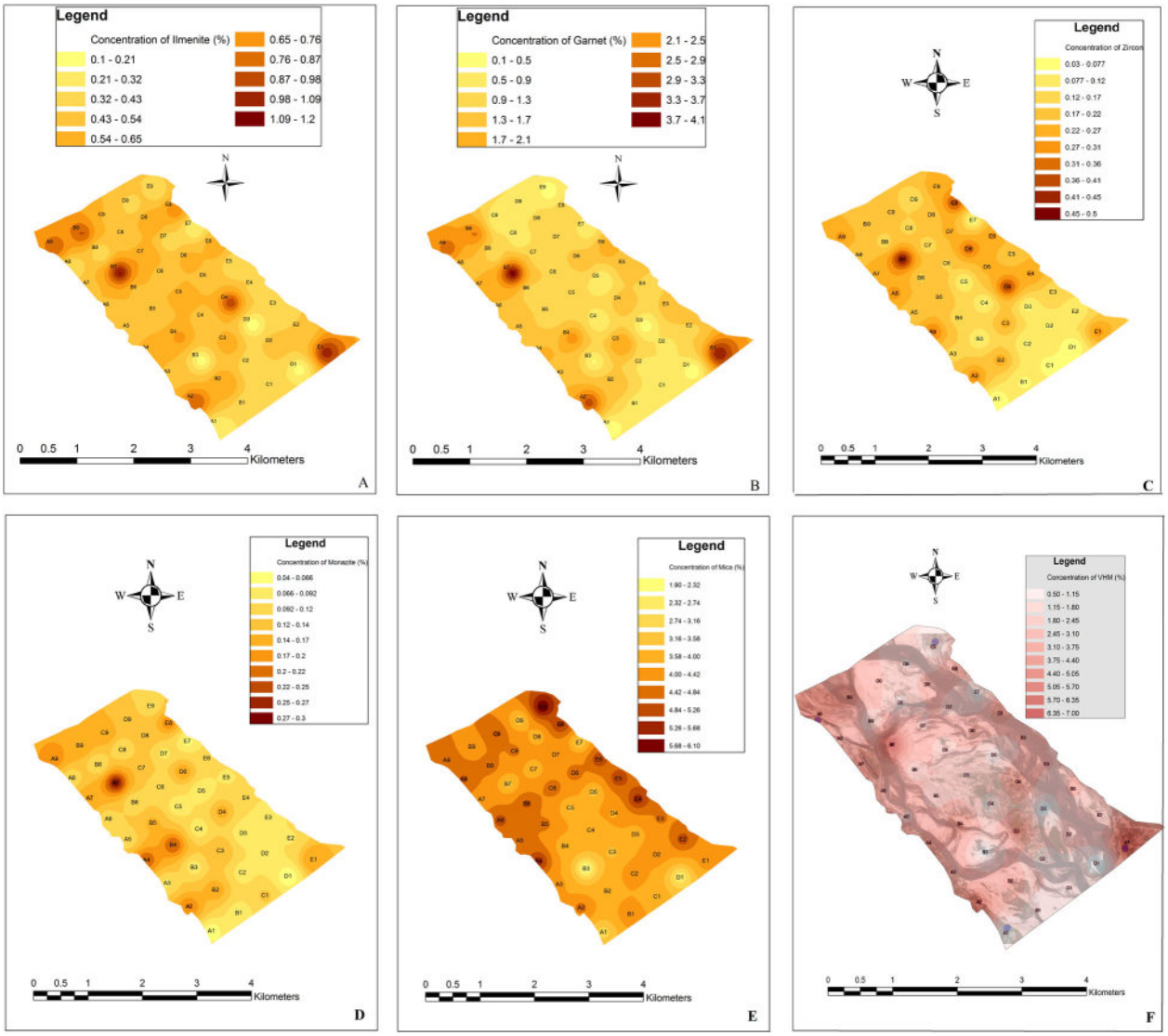

Figure 6. Concentration maps showing the distribution of various VHMC with depth for the 45 sample sites on the Rajpur mid-channel sand bar: (A) ilmenite; (B) garnet; (C) zircon; (D) monazite; (E) mica and (F) total VHMC.

and zircon products and a high-grade silica concentrate. Removal and recovery of the VHMCs also have additional benefits as sedimentary silica sand, being a common source for commercial silica, must be free of mica, organic matter, iron, titanium and trace elements.

The average content of total VHMs from various surface and borehole sample locations along the Tista river was consistently in the range 2–3wt-%. The VHMC comprised ilmenite, zircon, monazite, rutile, garnet, sillimanite and kyanite. Based on the results from the current study, the Rajpur mid-channel sand bar was selected as the region with the greatest concentration of sample data from which to derive preliminary resource estimation data.

The average HM content of the Rajpur mid-channel sand bar was 10.66% of which the VHMC comprised 2.51%. Resource maps based on the concentration of the different heavy minerals garnet, ilmenite, zircon, monazite and mica were prepared using an inverse distance weighting interpolation method by ArcGIS. In addition, a resource map showing the distribution of the combined VHM was also produced. These are shown in Figure 6.

The resource maps reflect the depositional process and mechanism of HM accumulations within the Rajpur mid-channel sand bar with the highest concentrations of VHMC at the bar head and margins compared to middle region and distal ends. These are regions where there is a reduction in flow velocity and represent preferred sites for the deposition of denser particles. The resource distribution maps also indicate the sand bar is cross-cut by a number of channels. These also appear to be sites at which there is a strong correlation with elevated HM accumulations. Large sand bars, therefore, represent key regions for investigation at other sites along the river as the accumulation of HM grains is responsible for flow separation within the alluvial channels causing abrupt changes in the bed geometry (e.g. Best and Brayshaw 1985). Based on the

laterally spaced samples, sand bars further upstream are most prospective as the concentrations of HMs generally increase upstream.

Summary

The distribution, mineralogy and abundance of VHMCs of the Tista river sediments were characterised as part of a broader project to examine the potential for the development of Tista river sediments as a recoverable by-product resource from sand mining. The most common particle size was between +125 to 500 μm with 84 wt-% of all material reporting to this size range. Laterally based surface sampling showed that the upstream component of the sand was characterised by a higher proportion of coarser particles, whereas finer particles increased downstream. Heavy liquid separation studies revealed that the concentration of HMs decreased with coarsening grain size. Analysis data from bore hole sampling indicated an overall coursing of the sand grain size with depth.

The Tista river sands are dominated by quartz with additional large amounts of 'light' aluminosilicate minerals including feldspars, micas and minor amounts of chlorite. HMs make up, on average, 10.99% of the sand samples and are composed primarily of amphiboles, garnets, pyroxenes and aluminosilicate (Al_2SiO_5) phases. The percentage of VHMs (ilmenite, rutile, zircon, monazite, garnet) was 2.47% in the bulk samples. Detailed sampling of a large mid-channel sand bar indicated a similar assemblage with an average HM content of 10.66% (VHMC = 2.51%). Resource mapping of the sand bar showed accumulations of HMs occurred upstream and along the margins of the bar thereby identifying sites for future prospectivity. Further work is in progress to conduct detailed mineral processing and characterisation studies to determine if the recoverable VHMC are easily extracted and are suitable for upgrading to more valuable products.

Acknowledgements

The authors wish to acknowledge the authority of BCSIR for approval of the project budget, CSIRO Mineral Resources for providing analytical support especially Dr Anita D'Angelo (CSIRO) for XRD analyses and also the staff of IMMM for their assistance. The authors also acknowledge the Project Director, Mineral Processing Center at IMMM of BCSIR for supporting the assignment of Pradip Biswas as a Visiting Scientist at CSIRO. This work was conducted as a part of the Ph.D. dissertation of Biswas, P.K.

Disclosure statement

No potential conflict of interest was reported by the authors.

References

Ahmed SS, Miah MY, Qumruzzaman C, Zaman MN, Badrul AAKM, Biswas PK. 2010. Alteration and exsolution characteristics of ilmenites of Moheskhali Island, Chittagong, Bangladesh. Bangladesh J Sci Ind Res. 45 (1):17–26.

Best JL, Brayshaw AC. 1985. Flow separation - a physical process for the concentration of heavy minerals within alluvial channels. J Geol Soc London. 142:747–755.

Blott SJ, Pye K. 2012. Particle size classes and classification of sediment types based on particle size distributions: review and recommended procedures. Sedimentology. 59:2071–2096.

Bruker AXS. 2013. TOPAS V5: general profile and structure analysis software for powder diffraction data. Version 5. Karlsruhe, Germany: Bruker AXS GmBH.

Chakraborty T, Ghosh P. 2010. The geomorphology and sedimentology of the Tista megafan, Darjeeling Himalaya: implications for megafan building processes. Geomorphology. 115:252–266.

Chowdhury MNM, Uddin S, Saleh S. 2014. Present scenario of renewable and non-renewable resources in Bangladesh: a compact analysis. Int J Sustain Green Energy. 3(6):164–178.

Degen T, Sadki M, Bron E, König U, Nénert G. 2014. The highscore suite. Powder Diffr. 29(S2):S13–S18.

Dill HG. 1998. A review of heavy minerals in clastic sediments with case studies from the alluvial-fan through the nearshore-marine environments. Earth-Sci Rev. 45:103–132.

Dill HG. 2007. Grain morphology of heavy minerals from marine and continental placer deposits, with special reference to Fe–Ti oxides. Sediment Geol. 198:1–27.

Gansser A. 1964. Geology of the Himalayas. New York (NY): Interscience Publishers; p. 289.

Garzanti E, Vezzoli G, Ando S, Lanord FG, Singh SK, Fosteret G. 2004. Sand petrology and focused erosion in collision orogens: the Brahmaputra case. Earth Planet Sc Lett. 220:157–174.

Ghosh K. 2015. Sandy macroforms dynamics and one dimensional facies characterization of the River Teesta. Indian J Geo Env Mang. 14:1–15.

Hill RJ, Howard CJ. 1987. Quantitative phase analysis from neutron powder diffraction data using the Rietveld method. J Appl Cryst. 20:467–474.

Hossain I, Ahmed SS, Islam N, Biswas PK, Rahman MA. 2013. Glass sand potentiality of bar sediments from Tista and Dharla rivers, Bangladesh. Rajshahi University J Life Earth Agr Sci. 41:57–64.

ICDD. 2016. PDF-4 powder diffraction database. Newtown Square (PA): International Centre for Diffraction Data.

Islam MA. 1997. Areal variation of monazite, zircon, magnetite and ilmenite in Cox's Bazar, Bangladesh. J Indian Assoc Sedimentologists. 16:243–247.

Kabir MZ, Deeba F, Rajib M. 2006. Optical and mineralogical characteristics of some major beach placer minerals of Bangladesh; Technical report, BSMEC/TR-1/2006, February'06, Beach Sand Minerals Exploitation Center, Bangladesh Atomic Energy Commission, Cox's Bazar, Bangladesh.

Khan SS, Islam TAR. 2015. Anthropogenic impact on morphology of Teesta River in Northern Bangladesh: an exploratory study. J Geosci Geomat. 3:50–55.

Kundu A, Matin A, Muku IM. 2012. Depositional environment and provenance of Middle Siwalik sediments in

Tista valley, Darjiling District, Eastern Himalaya, India. J Earth Syst Sci. 121:73–89.
Mange MA, Maurer HFW. 1992. Heavy minerals in colour. London: Chapman and Hall; p. 147.
Mitra S, Ahmed SS, Moon H-S. 1992. Mineralogy and chemistry of the opaques of Cox's Bazar (Bangladesh) beach sands and the oxygen fugacity of their provenance. Sediment Geol. 77:235–247.
Morton AC. 1991. Geochemical studies of detrital heavy minerals and their application to provenance research. In: Morton AC, Todd SP, Haughton PDW, editors. Developments in sedimentary provenance studies. Special Publication 57. London: Geological Society of London, p. 31–46.
Morton AC, Hallsworth CR. 1999. Processes controlling the composition of heavy mineral assemblages in sandstones. Sediment Geol. 124:3–29.
Mukhopadhyay SC. 1982. The Tista Basin: a study of fluvial geomorphology. In: Bagchi KP, editor. The Ganges delta. Calcutta: University of Calcutta Press; p. 157.
Rahman MA, Biswas PK, Zaman MN. 2014. River sands of Bangladesh. Saarbrucken, Germany: Lap Lambert Academic Publishing, AV Akademikerverlag GmbH & Co, KG; p. 1–73.
Rahman MA, Pownceby MI, Haque N, Bruckard WJ, Zaman MN. 2016. Valuable heavy minerals from the Brahmaputra River sands of Northern Bangladesh. Trans IMM Section B. 125:174–188.
Rahman MA, Zaman MN, Biswas PK, Sultana MS. 2017. Economic viability of the Tista River sand deposits in Bangladesh, an overview. J Sci Res. 9(2):219–233.
Rajib M, Kabir MZ, Deeba F, Zaman MM, Rana SM. 2007. Distribution of five major heavy minerals along the recent beach areas of Bangladesh. Bangladesh J NOAMI. 24(1): P-1–P-9.
Rietveld HM. 1969. A profile refinement method for nuclear and magnetic structures. J Appl Cryst. 2:65–71.
Vezzoli G, Lombardo B, Rolfo F. 2017. Petrology of the Tista and Rangit river sands (Sikkim, India). Ital J Geosci. 136:103–109.
Zaman MN, Rahman MA, Biswas PK. 2012. Sands of the Brahmaputra river basin Bangladesh. Saarbrucken, Germany: Lap LAMBERT Academic Publishing, AV Akademikerverlag GmbH & Co. KG, p.12.